Article

J. Mex. Chem. Soc. **2007**, *51(1)*, 20-26

ISSN 1870-249X

CF_3S-Platinum(II) Complexes with Fluorinated Dithioethers. Molecular Structures of $[Pt(SCF_3)_2(R_fSCH_2CH_2SR_f)]$ $R_f = C_6H_4F$-2 and C_6H_4F-3

Ruy Cervantes,[1] Ubaldo Duran,[1] Sylvain Bernès[2] and Hugo Torrens[1]*

[1] Facultad de Química, Universidad Nacional Autónoma de México. Ciudad Universitaria 04510, México D.F., Mexico. Tel/fax (55)56223724, torrens@servidor.unam.mx

[2] Facultad de Ciencias Químicas, Universidad Autónoma de Nuevo León, Ciudad Universitaria, 66451 S. Nicolás de los Garza, Nuevo León, Mexico.

Recibido el 4 de agosto del 2006; aceptado el 24 de noviembre del 2006

Abstract. This paper describes the synthesis and characterization of the platinum(II) compounds *cis*-$[Pt(SCF_3)_2(R_fSCH_2CH_2SR_f)]$ R_f = C_6F_5 **1**, C_6HF_4-4 **2**, C_6H_4F-2 **3**, C_6H_4F-3 **4**, C_6H_4F-4 **5** and $C_6H_4(CF_3)$-3 **6**. Variable temperature ^{19}F NMR spectra of these complexes, show the presence and interconvertion of *syn* and *anti* isomers, consistent with a fast flipping of the metalocycle ring and a slow inversion of configuration at the dithioether sulfur atoms. The molecular and crystalline structures of the compounds $[Pt(SCF_3)_2(2\text{-}C_6H_4FSCH_2CH_2SC_6H_4F\text{-}2)]$ **3** and $[Pt(SCF_3)_2(3\text{-}C_6H_4FSCH_2CH_2SC_6H_4F\text{-}3)]$ **4**, solved by X-ray diffraction are also described.
Key words: fluorothiols, fluorothioetheres, platinum, VT-NMR, X-ray.

Resumen. En este artículo se describen la síntesis y caracterización de los compuestos de platino(II) *cis*-$[Pt(SCF_3)_2(R_fSCH_2CH_2SR_f)]$, R_f = C_6F_5 **1**, C_6HF_4-4 **2**, C_6H_4F-2 **3**, C_6H_4F-3 **4**, C_6H_4F-4 **5** y $C_6H_4(CF_3)$-3 **6**. Para estos compuestos, los espectros de RMN de ^{19}F obtenidos a diferentes temperaturas, muestran la presencia e interconversión de isómeros *syn* y *anti*, consistente con un cambio conformacional rápido del metalociclo y una inversión de configuración lenta en los átomos de azufre del ditioeter. Se describen también las estructuras cristalinas y moleculares de los compuestos $[Pt(SCF_3)_2(2\text{-}C_6H_4FSCH_2CH_2SC_6H_4F\text{-}2)]$ **3** y $[Pt(SCF_3)_2(3\text{-}C_6H_4FSCH_2CH_2SC_6H_4F\text{-}3)]$ **4**, determinadas mediante difracción de rayos-X.
Palabras clave: Fluorotioles, fluorotioéteres, platino RMN-TV, Rayos X

Introduction

The coordination chemistry of thiolates with platinum group metals has developed extensively over the last few decades [1,2]. This set of complexes have played an important role in areas such as bioinorganic chemistry, synthesis and catalysis [3-18]. On the other hand, the analogous relatively younger chemistry focused on the fluorine-containing homologues is still developing.[9].

It is well known that organo-sulfur compounds tend to act as bridging ligands which frequently renders them unsuitable for preparing mononuclear complexes. Thiolate monometallic complexes can be stabilized with strong bonding auxiliary ligands reluctant to substitution such as a chelated ligand; by reducing the coordination capability of the thiolate ligands (for example by using fluorine atoms because of their electron-withdrawing effects), rendering them unable to displace other ligands at the metallic center or by a measured combination of these two factors. Therefore, transition metal complexes bearing thiolato ligands are useful and versatile building blocks for the synthesis of higher nuclearity derivatives with either homo- or hetero-metallic centers [10].

The dynamic behavior exhibited by compounds with general formula $[M(SR)_2(R'SR''SR')]$ (R'SR''SR' = chelating thioether ligand) has been found to arise from two main processes: ring flipping and inversion of configuration at sulfur chelating thioether.

Three coordinated sulfur atom can change its configuration through a sulfur inversion process, giving *anti* and *syn* isomers. Its activation energy is affected by different factors [11] such as *trans* influence, the nature of the inversion center, the nature of the metallic center and π conjugation in the ligands.

In order to further explore the chemistry of $[M(SR)_2(R'SR''SR')]$ compounds, the preparation and characterization of a variety of platinum complexes with chelating dithioethers, as a fixed auxiliary ligand, and CF_3S^-, have been undertaken.

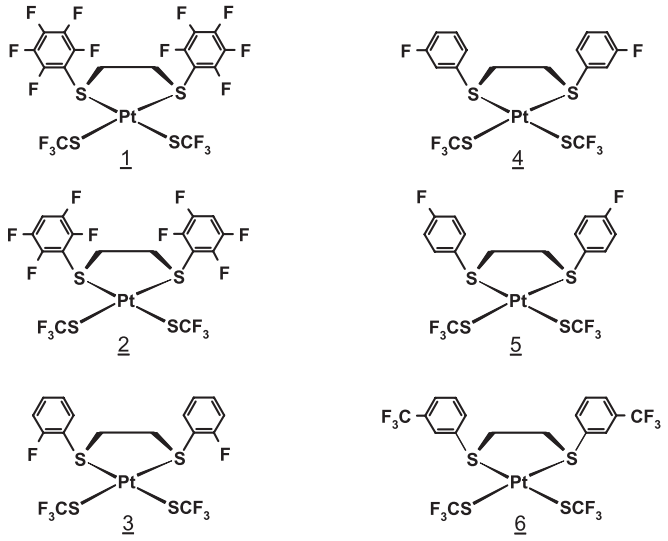

Scheme 1

In this paper the following platinum(II) complexes, see scheme 1, are reported: *cis*-[Pt$(SCF_3)_2(R_fSCH_2CH_2SR_f)$] R_f = C_6F_5 **1**, C_6HF_4-4 **2**, C_6H_4F-2 **3**, C_6H_4F-3 **4**, C_6H_4F-4 **5** and $C_6H_4(CF_3)$-3 **6**. We have studied the dynamic behavior of these complexes using ^{19}F-{^1H} NMR. The crystal and molecular structures of [Pt$(SCF_3)_2$(2-$C_6H_4FSCH_2CH_2SC_6H_4F$-2)] **3** and [Pt$(SCF_3)_2$(3-$C_6H_4FSCH_2CH_2SC_6H_4F$-3)] **4**, solved by X-ray diffraction are also described.

Results and Discussion

Compounds formulated as [$PtX_2(RSCH_2CH_2SR)$] can give rise to isomers **A**, **B** and **C**, as shown in Fig. 1, due to the relative mutual position of the sulfur substituents and the configuration at the PtS_2C_2 ring.

Normally, at room temperature and in solution, isomers **B** and **C** can not be distinguished using NMR since the PtS_2C_2 ring is flipping faster than the spectroscopic time involved. Only few examples are known in which bulky substituents R allow detection of the -SCR_2CR_2S- configurations at very low temperatures [12] but only the dynamic average of both stereoisomers **B** and **C** in Fig. 1 can usually be observed.

On the other hand, isomers *syn* and *anti* in Fig. 1, can also be interconverted trough a process known as inversion of configuration at the sulfur atoms. The energy range for sulfur inversion is found between 40 and 80 kJmol^{-1} and therefore both isomers can normally be experimentally observed at room temperature by NMR experiments [13].

IR spectra of compounds **1**-**6** show the expected absorptions arising from the common CF_3S^- ligand and the corresponding dithioether ligand present in each compound.

In terms of NMR, the magnetic systems corresponding to the fluorinated rings can be described as follows: C_6F_5 AA'BB'C, C_6HF_4-4 and C_6H_4F-4 AA'BB'X, C_6H_4F-2, and C_6H_4F-3 ABCDX and $C_6H_4(CF_3)$-2 $ABCDX_3$ respectively. All magnetic systems are of second order and experimentally spectra exhibit complex signals. ^{19}F-{^1H} NMR parameters for compounds **1** to **6**, in agreement with the descriptions above, are listed in the experimental section.

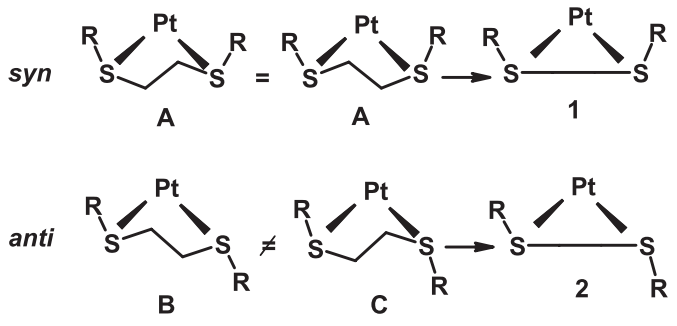

Fig. 1. *Syn* (**A**) and *anti* (**B** and **C**) isomers derived from a dynamic ligand $RSCH_2CH_2SR$, and *syn* (**1**) and *anti* (**2**) isomers from an averaged $RSCH_2CH_2SR$ ligand.

Metathesis reactions of [$PtCl_2(R_fSCH_2CH_2SR_f)$] R_f = C_6F_5, C_6HF_4-4, C_6H_4F-2, C_6H_4F-3, C_6H_4F-4 and $C_6H_4(CF_3)$-3. with silver trifluoromethyl-thiolate (equation 1) afford the desired complexes **1** to **6**.

$$[PtCl_2(R_fSCH_2CH_2SR_f)] + 2\ Ag(SCF_3) \rightarrow [Pt(SCF_3)_2(R_fSCH_2CH_2SR_f)] + 2\ AgCl \quad (1)$$

R_f = C_6F_5 **1**, C_6HF_4-4 **2**, C_6H_4F-2 **3**, C_6H_4F-3 **4**, C_6H_4F-4 **5** and $C_6H_4(CF_3)$-3 **6**.

Compounds [Pt$(SCF_3)_2(C_6F_5SCH_2CH_2SC_6F_5)$] **1** and [Pt$(SCF_3)_2(C_6HF_4SCH_2$-$CH_2SC_6HF_4)$] **2** are rather unstable, decompose rapidly (min) in solution at room temperature and almost immediately when warmed up. ^{19}F-{^1H} NMR experiments show the presence of the free dithioether ligand and insoluble polymeric [14] solids among the decomposition products, as shown in equation 2.

$$n\ [Pt(SCF_3)_2(R_fSCH_2CH_2SR_f)] \rightarrow n\ R_fSCH_2CH_2SR_f + (Pt(SCF_3)_2)_n \quad (2)$$

R_f = C_6F_5 **1**, C_6HF_4-4 **2**

Compounds **3** to **6** were obtained as stable, diamagnetic yellow microcrystalline solids, soluble in acetone, dichloromethane and chloroform.

Room temperature ^{19}F-{^1H} NMR spectra of compounds **1** to **6** in the CF_3S^- region exhibit a broad distorted singlet with ^{195}Pt satellites due to overlapping signals in agreement with the presence of *syn* and *anti* isomers (**1** and **2** in Fig. 1). The presence of only two isomers indicates that conformational changes due to ring flipping are very fast in the NMR time scale; otherwise, if ring conformers were distinguishable, tree isomers would be detected.

It is not possible to distinguish which one of the two ^{19}F-{^1H} NMR signals observed, corresponds to the *syn* and which to the *anti* isomers. It has been found before [12,15] that the more abundant isomer is frequently the *anti* conformer since steric interaction among aromatic substituents in an *anti* configuration is much less than in the *syn* configuration. Furthermore, in the solid state compounds **3** to **5**, *vide infra*, crystallize with the *anti* configuration.

At room temperature both, *syn* and *anti* isomers, are in equilibrium, Fig 2, with different relative abundances. The rate of interconvertion in this equilibrium increases with the temperature. A further point worth noticing is that the presence of two signals on the ^{19}F-{^1H} NMR spectra implies that the inversion of configuration is not solely and simultaneously on both sulfur atoms.

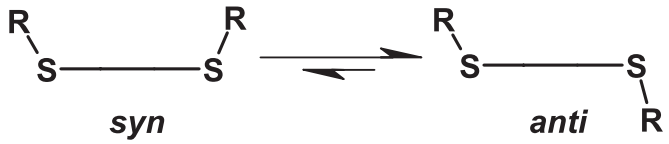

Fig. 2. Equilibrium in the interconvertion of *syn* and *anti* isomers - from an averaged SCH_2CH_2S fragment-usually shifted to the right.

Room temperature ^{19}F-{^{1}H} NMR spectra of the unstable compounds [Pt(SCF_3)$_2$($C_6F_5SCH_2CH_2SC_6F_5$)] **1** and [Pt(SCF_3)$_2$(4-$C_6HF_4SCH_2CH_2SC_6HF_4$-4)] **2**, prepared on the NMR tube immediately before measurements, exhibit a relatively broad singlet with ^{195}Pt satellites in the CF_3S^- region (δ = -27.19, $^3J_{Pt\text{-}F}$ = 112.01 and -27.10 ppm, $^3J_{Pt\text{-}F}$ = 101.15 respectively) and the corresponding signals from the SC_6F_5 and SC_6F_4H-4 moieties, together with signals arising from decomposition products.

Variable temperature NMR. At 40 °C the ^{19}F-{^{1}H} NMR spectra of compounds **3** to **6** in the CF_3S^- region, show a singlet with ^{195}Pt satellites, see Fig. 3, suggesting a fast interconvertion of *syn* and *anti* isomers. **3**: ^{19}F δ = -27.03 ppm, $^3J_{Pt\text{-}F}$ = 93.91 Hz; **4**: ^{19}F δ = -27.92 ppm, $^3J_{Pt\text{-}F}$ = 92.73 Hz; **5**: ^{19}F δ = -27.58 ppm, $^3J_{Pt\text{-}F}$ = 92.98 Hz; **6**: ^{19}F δ = -26.92 ppm, $^3J_{Pt\text{-}F}$ = 92.54 Hz. On cooling down, the CF_3S singlet collapses into two signals, isomers A and B, which are driven away until -50°C where two signals with ^{195}Pt satellites are clearly differentiated. **3A**: ^{19}F δ = -27.21 $^3J_{Pt\text{-}F}$ = 96.55 Hz; and **3B** δ = -27.60 ppm, $^3J_{Pt\text{-}F}$ = 92.74 Hz; **4A**: ^{19}F δ = -27.25 $^3J_{Pt\text{-}F}$ = 96.63 Hz; and **4B** -27.64 ppm, $^3J_{Pt\text{-}F}$ = 93.01 Hz; **5A**: ^{19}F δ = -27.28 $^3J_{Pt\text{-}F}$ = 96.90 Hz; and **5B** -27.67 ppm, $^3J_{Pt\text{-}F}$ = 93.12 Hz; **6A**: ^{19}F δ = -27.34 $^3J_{Pt\text{-}F}$ = 89.77 Hz; and **3B** δ = -27.76 ppm, $^3J_{Pt\text{-}F}$ = 94.86 Hz. The relative abundances of isomer A:isomer B are ≈10:1 for all compounds **3** to **6**.

The free enthalpy of activation ($\Delta G^{\ddagger}$) involved in inversion of configuration depends on the metallic center, on the type of sulfur substituents and on the nature of the substituents *trans* to the inverting sulfur atom. $\Delta G^{\ddagger}$, defined by the Eyring equation, depends directly on the coalescence temperature (T_C) at which the signals of two isomers merge into a single resonance as the velocity (K_C) of the inversion increases. A relatively large coalescence temperature indicates a comparatively large energetic barrier for the inversion process. Table 1 collects the coalescence temperatures found for compounds **3** to **6** as well as comparative data from the literature.

As can be seen from the values on Table 1, coalescence temperatures decrease as the *trans*-effect of the anionic ligand increases ($Cl^- < Br^- < I^-$). We have found that compounds **3** to **6** have relatively very low coalescence temperatures, around 15 °C, suggesting a relatively high *trans*-effect of the CF_3S group, as has been pointed out previously [18]. On the other hand, the coalescence temperature increases with the electronegativity at the sulfur substituent, probably because the intermediate (sp^2 + p)-p, considered in the postulated inversion mechanism, is favored. In this work however all four substituents involved (R = C_6H_4F-2, C_6H_4F-3, C_6H_4F-4, $C_6H_4(CF_3)$-3) seem to have practically the same electronegativity.

Molecular structures. Figs. 4 and 5 show ORTEP-like [19] representations of the molecular structures of [Pt(SCF_3)$_2$(2-$C_6H_4FSCH_2CH_2SC_6H_4F$-2)] **3**, and [Pt(SCF_3)$_2$(3-$C_6H_4FSCH_2CH_2SC_6H_4F$-3)] **4**. Main bond distances and angles are quoted in Table 2.

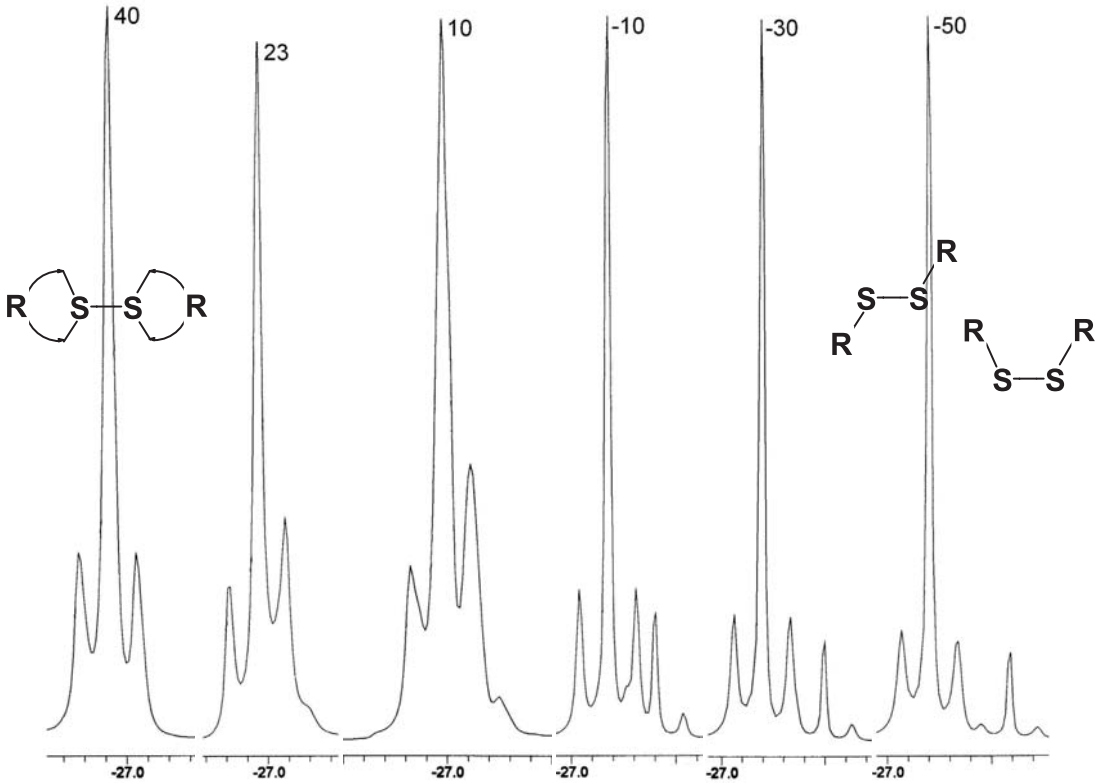

Fig. 3. Variable temperature (°C) ^{19}F-{^{1}H} NMR spectra of compound [Pt(SCF_3)$_2$(2-$C_6H_4FSCH_2CH_2SC_6H_4F$-2)] **3**, showing the SCF_3 region. On the left, the representation of a very fast exchange of R positions.

Table 1. Coalescence temperatures of selected $[PtX_2(RSCH_2CH_2SR)]$ compounds.

Compound	Temp °C	Ref.
$[PtCl_2(CF_3SCH_2CH_2SCF_3)]$	130	12
$[PtCl_2(MeSCH_2CH_2SMe)]$	100	16
$[PtCl_2(EtSCH_2CH_2SEt)]$	80	16
$[PtCl_2(^nPrSCH_2CH_2S^nPr)]$	95	16
$[PtCl_2(^nBuSCH_2CH_2S^nBu)]$	92	16
$[PtCl_2(MeSCH_2CH_2SMe)]$	100	16
$[PtBr_2(MeSCH_2CH_2SMe)]$	93	16
$[PtI_2(MeSCH_2CH_2SMe)]$	87	16
$[Pt(SCF_3)_2(2\text{-}C_6H_4FSCH_2CH_2SC_6H_4F\text{-}2)]$ **3**	15	This work
$[PtCl_2(2\text{-}C_6H_4FSCH_2CH_2SC_6H_4F\text{-}2)]$	84	17
$[Pt(SCF_3)_2(3\text{-}C_6H_4FSCH_2CH_2SC_6H_4F\text{-}3)]$ **4**	16	This work
$[PtCl_2(3\text{-}C_6H_4FSCH_2CH_2SC_6H_4F\text{-}3)]$	73	17
$[Pt(SCF_3)_2(4\text{-}C_6H_4FSCH_2CH_2SC_6H_4F\text{-}4)]$ **5**	15	This work
$[PtCl_2(4\text{-}C_6H_4FSCH_2CH_2SC_6H_4F\text{-}4)]$	77	17
$[Pt(SCF_3)_2(3\text{-}C_6H_4(CF_3)SCH_2CH_2SC_6H_4(CF_3)\text{-}3]$ **6**	15	This work
$[PtCl_2(3\text{-}C_6H_4(CF_3)SCH_2CH_2SC_6H_4(CF_3)\text{-}3]$	78	17
$[Pt(SC_6F_5)_2(2\text{-}C_6H_4FSCH_2CH_2SC_6H_4F\text{-}2))]$	40	17
$[Pt(SC_6F_5)_2(3\text{-}C_6H_4FSCH_2CH_2SC_6H_4F\text{-}3)]$	32	17
$[Pt(SC_6F_5)_2(4\text{-}C_6H_4FSCH_2CH_2SC_6H_4F\text{-}4)]$	37	17
$[Pt(SC_6F_5)_2(3\text{-}C_6H_4(CF_3)SCH_2CH_2SC_6H_4(CF_3)\text{-}3)]$	35	17
$[Pt(p\text{-}SC_6HF_4)_2(2\text{-}C_6H_4FSCH_2CH_2SC_6H_4F\text{-}2)]$	27	17
$[Pt(p\text{-}SC_6HF_4)_2(3\text{-}C_6H_4FSCH_2CH_2SC_6H_4F\text{-}3)]$	26	17
$[Pt(p\text{-}SC_6HF_4)_2(4\text{-}C_6H_4FSCH_2CH_2SC_6H_4F\text{-}4)]$	32	17
$[Pt(p\text{-}SC_6HF_4)_2(3\text{-}C_6H_4(CF_3)SCH_2CH_2SC_6H_4(CF_3)\text{-}3)]$	28	17

Table 2. Main geometric parameters in **3** and **4**.

Coordination bond lengths (Å)			
3		**4**	
Pt1 S1	2.3345(10)	Pt1 S1	2.3252(15)
Pt1 S2	2.2939(11)	Pt1 S2	2.3041(15)
Pt1 S3	2.3052(10)	Pt1 S3	2.3052(13)
Pt1 S4	2.3051(9)	Pt1 S4	2.3028(15)
Selected bond angles (°)			
3		**4**	
S1 Pt1 S2	82.63(4)	S1 Pt1 S2	83.15(6)
S1 Pt1 S3	89.64(4)	S1 Pt1 S3	89.07(5)
S1 Pt1 S4	178.59(4)	S1 Pt1 S4	176.49(5)
S2 Pt1 S3	172.27(4)	S2 Pt1 S3	172.17(5)
S2 Pt1 S4	98.55(4)	S2 Pt1 S4	98.54(6)
S3 Pt1 S4	89.18(4)	S3 Pt1 S4	89.28(5)
C1 S1 Pt1	101.41(16)	C1 S1 Pt1	101.4(3)
C2 S2 Pt1	111.60(16)	C2 S2 Pt1	109.7(2)

Both complexes have very similar molecular structures, as reflected in the small r.m.s. difference of 0.042 Å for overlayed structures (deviation computed using Pt and S atoms). Thus, the position of F atoms for the bidentate ligand has little influence on the molecular conformation. Pt(II) ions are coordinated by four S atoms, with Pt-S bond lengths spanning a short range around the expected value of *ca*. 2.30 Å. However, in contrast with the close similarity of these bond distances, the basicity of the groups R_fS and CF_3S are considered highly different and, on this ground, one would expect larger CF_3S-Pt bond distances. The apparent shortening of the $(CF_3)S$-Pt bond has been explained considering that CF_3S is a highly effective competitor for metal to ligand π back donation [20], but this matter still remains controversial [18].

The coordination geometry approximates a square, as found in the vast majority of structurally characterized four-coordinated Pt(II) complexes. The smaller *cis* S-Pt-S angle involves CF_3S ligands [**3**: 82.63(4)º; **4**: 83.15(6)º], while the larger corresponds to a $(CF_3)S$-Pt-SR_f fragment [**3**: 98.55(4)º; **4**: 98.54(6)º]. These deviations from an ideal square planar arrangement are clearly related to steric hindrances induced by the conformation stabilized in the solid state for **3** and **4**. Aryl substituents on S3 and S4 atoms occupy alternated

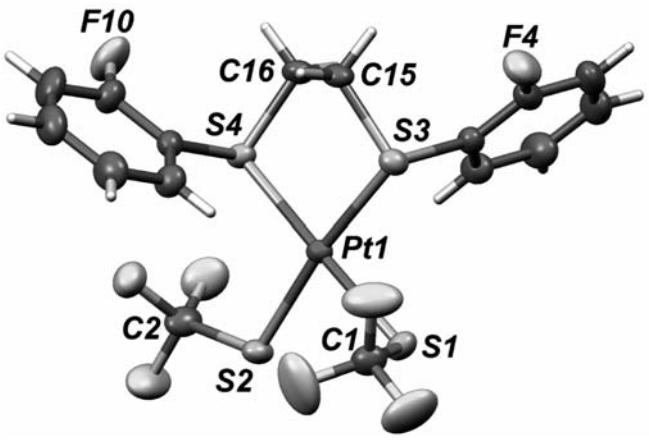

Fig. 4. ORTEP-like representation of compound [Pt(SCF_3)$_2$(2-$C_6H_4FSCH_2CH_2SC_6H_4F$-2)] **3** with displacement ellipsoids for non-H atoms at the 30% probability level.

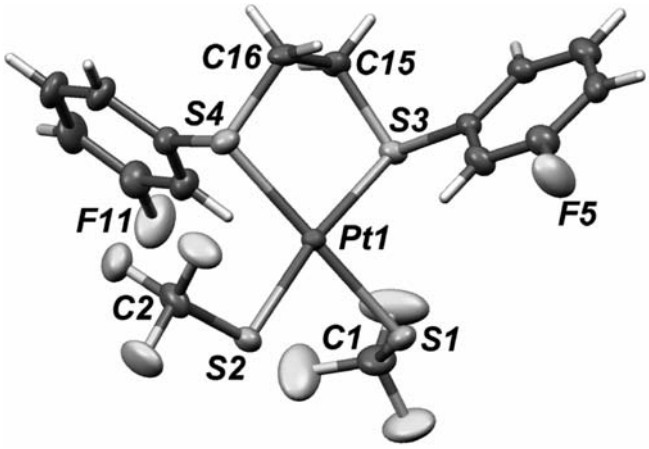

Fig. 5. ORTEP-like representation of compound [Pt(SCF_3)$_2$(3-$C_6H_4FSCH_2CH_2SC_6H_4F$-3)] **4** with displacement ellipsoids for non-H atoms at the 30% probability level.

positions relatively to the S1/S2/S3/S4 plane of each molecule, with an *anti* configuration, minimizing steric interactions for the bidentate ligands. This configuration is presumably that corresponding to the main isomer present in solution, as observed by ^{19}F-{^1H} NMR. Although the configuration commonly encountered for this class of ligands is the *anti*, the solid state structures of structurally related complexes [$PtCl_2(CF_3SCH(CH_3)CH_2SCF_3)$], [12] [$PtCl_2(CH_3SCH(CF_3)CH(CF_3)SCH_3)$], [21] [$Pt(SC_6F_5)_2(CH_3SCH(CH_3)CH(CH_3)SCH_3)$] [22] and [$PtCl_2(CH_3SCF_2CH_2SCH_3)$] [23], with far smaller thioether-sulfur substituents, exhibit the *syn* configuration. Thus, for a given molecule including such ligands, both *anti* and *syn* configurations may be expected in solution, while a single configuration should be stabilized in the solid state, as observed in the present work.

The C-S-Pt angles, ranging from 101.41(16) to 111.60(16)º in **3** and from 101.4(3) to 109.7(2)º in **4**, suggest that the geometries around the S atoms are pyramidal, nearly tetrahedral. Each S atom can then be considered as being sp^3 hybridized, regardless of valence for these atoms.

A worth notice feature on these compounds is the fact that the crystal structures seem to be controlled by the substitution on the benzene groups: the position of the F atoms, in *ortho* or *para*, determines intermolecular interactions, which, in turn, allows to change the crystal symmetry from *P*1 to $P2_1/c$ (see Table 3), although molecular structures are almost identical. In the case of **3** (triclinic symmetry), short F...H and S...H intermolecular contacts are observed, the shortest separations being F...H = 2.566 Å and S...H = 2.880 Å, while F atoms substituting the benzene rings are not involved in significant interactions (Fig. 6). A different behavior is observed in the case of **4**, where the *meta*-F atom F5 gives a contact with a neighboring benzene ring, F5...H4A = 2.461 Å, as a weak contact with a S atom, F5...S1 = 3.258 Å. The resulting centrosymmetric dimer is further connected with symmetry related molecules, through CF_2F...H and S...H contacts, giving a bidimensional network (Fig. 7).

Experimental part

All reagents were purchased from Aldrich and used as received. [$PtCl_2(R_fSCH_2CH_2SR_f)$], (R_f = C_6F_5, C_6HF_4-4, C_6H_4F-2, C_6H_4F-3, C_6H_4F-4 and $C_6H_4(CF_3)$-3) [12,24] and $AgSCF_3$, [25], were prepared by published methods.

All reactions were carried out under an atmosphere of dry, oxygen-free N_2(g) using Schlenk techniques. Solvents

Table 3. Crystal data for **3** and **4**.

Compound	3	4
Empirical Formula	$C_{16}H_{12}F_8PtS_4$	$C_{16}H_{12}F_8PtS_4$
Space group	*P*‘1	$P2_1/c$
a, Å	8.2213 (8)	7.9357 (9)
b, Å	8.5025 (7)	33.633 (3)
c, Å	17.5451 (14)	8.6050 (10)
a, º	79.086 (7)	
b, º	87.878 (7)	116.850 (10)
g, º	61.115 (6)	
V, Å^3	1052.31 (16)	2049.1 (4)
Z	2	4
r_{calc}, g.cm^{-3}	2.145	2.203
m, mm^{-1}	7.133	7.326
l, Å	0.71073	0.71073
$2q_{max}$, º	60	56
T, K	296	296
R_1[a] %	2.84	3.49
wR_2[b] %	6.78	8.58
Data / parameters	6097 / 262	4932 / 263

[a]$R=\Sigma||F_o|-|F_c||/\Sigma|F_o|$. [b]$wR_2=[\Sigma w(|F_o|-|F_c|)^2/\Sigma w|F_o|^2]^{1/2}$.

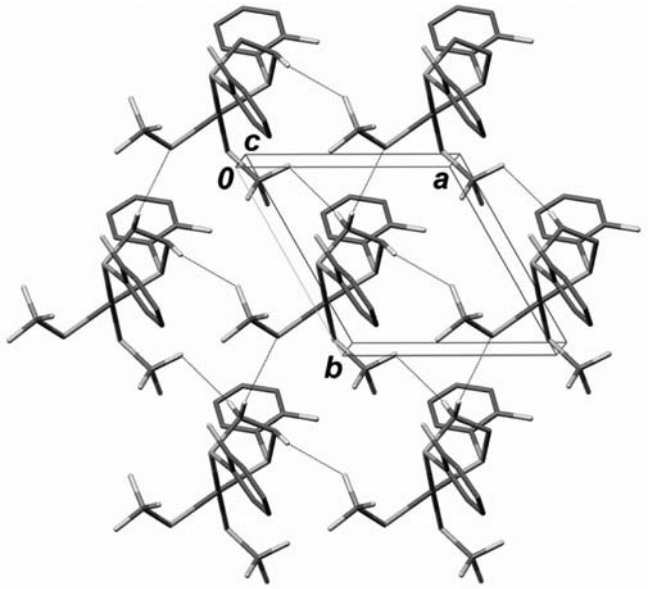

Fig. 6. Part of the crystal structure of $[Pt(SCF_3)_2(2\text{-}C_6H_4FSCH_2CH_2SC_6H_4F\text{-}2)]$ **3** viewed along [001], showing intermolecular contacts (thin blue lines). For the sake of clarity, H atoms not involved in contacts have been omitted.

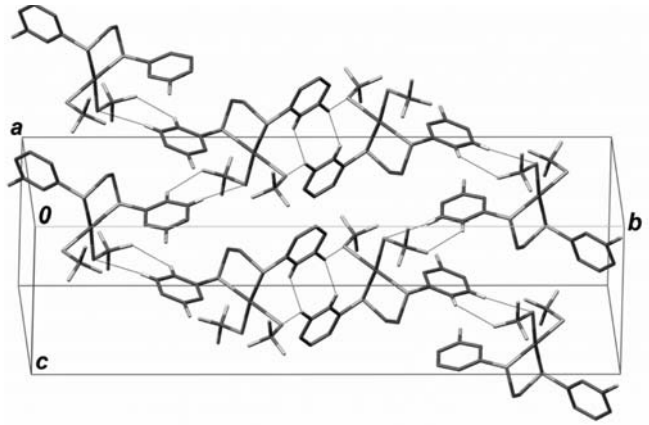

Fig. 7. part of the crystal structure of $[Pt(SCF_3)_2(3\text{-}C_6H_4FSCH_2CH_2SC_6H_4F\text{-}3)]$ **4**, showing intermolecular (thin blue lines). For the sake of clarity, H atoms not involved in contacts have been omitted.

were dried and degassed prior to use, using standard techniques [26].

Microanalyses were performed using a Fisons EA1108 instrument. ^{19}F-{^1H} NMR spectra were recorded on a Varian NT360 spectrometer operating at 282.23 MHz by Spectral Data Services Inc (Illinois USA.) on D_6-acetone solutions. Chemical shifts are in ppm relative to $CFCl_3$ (for ^{19}F) at 0 ppm, positives to low field and referenced to residual partially deuterated solvent peaks; coupling constants are in hertz (Hz). A standard variable-temperature unit was used to control the probe temperature and this was checked periodically using a thermocouple to ensure temperature readings were within 1 ^oC. Complexes were dissolved in deuterated acetone. The IR spectra were measured on a Nicolet Avatar FT-IR spectrometer as CsI pellets.

The experimental procedure for the preparation of compounds **1** t **6** is exemplified with the following general procedure:

$[Pt(SCF_3)_2(R_fSCH_2CH_2SR_f)]$. To a solution of the corresponding complex $[PtCl_2(R_fSCH_2CH_2SR_f)]$ (0.3 mmol) in acetone (50 cm^3) were added two equivalents of $AgSCF_3$ (0.6 mmol) in acetone (15 cm^3). The mixture was stirred for 3 h and filtered on Celite to remove the AgCl. The resulting yellow solution was evaporated to 20 cm^3 and the product precipitated with hexane, filtered and dried under vacuum at room temperature. Crystals were growth by slow evaporation of acetone solution.

$[Pt(SCF_3)_2(C_6F_5SCH_2CH_2SC_6F_5)]$ 1. NMR tube synthesis. ^{19}F-{H} NMR (C_3D_6O, 296K): δ (ppm) -125.53(m, F_{ortho}, 2), -159.16 (m, F_{meta}, 2), -122.60 (tt, F_{para}, 1), -27.19 (s+d, F_{SCF3}, $^3J_{Pt\text{-}F}$ = 112.01 Hz, 3).

$[Pt(SCF_3)_2(4\text{-}C_6HF_4SCH_2CH_2SC_6HF_4\text{-}4)]$ 2. NMR tube synthesis. ^{19}F-{H} NMR (C_3D_6O, 296K): δ (ppm) -122.47(m, F_{ortho}, 2), -133.45 (m, F_{meta}, 2), -27.10 (s+d, F_{SCF3}, $^3J_{Pt\text{-}F}$ = 101.15 Hz, 3).

$[Pt(SCF_3)_2(2\text{-}C_6H_4FSCH_2CH_2SC_6H_4F\text{-}2)]$ 3. Yellow solid, Yield: 177 mg (87%). ^{19}F-{H} NMR (C_3D_6O, 296K): δ (ppm) -108.16(m, F_{ortho}, 2), -26.95 (s+d, F_{SCF3}, $^3J_{Pt\text{-}F}$ = 87.06 Hz, 3). ^{19}F-{H} NMR (C_3D_6O, 223K): δ (ppm), **3A** -108.16(m, F_{ortho}, 2), -27.21 (s+d, F_{SCF3}, $^3J_{Pt\text{-}F}$ = 96.55 Hz, 3) **3B** -108.36(m, F_{ortho}, 2), -27.60 (s+d, F_{SCF3}, $^3J_{Pt\text{-}F}$ = 92.74 Hz, 3). Anal. Calcd. for $C_{16}H_{12}F_8PtS_4$: C 28.28; H 1.78; S 18.87. Found: C 28.4; H 1.5; S 18.6.

$[Pt(SCF_3)_2(3\text{-}C_6H_4FSCH_2CH_2SC_6H_4F\text{-}3)]$ 4. Yellow solid, Yield: 173 mg (85%). ^{19}F-{H} NMR (C_3D_6O, 296K): δ (ppm) -108.7 (m, F_{meta}, 2), -27.01 (s+d, F_{SCF3}, $^3J_{Pt\text{-}F}$ = 92.22 Hz, 3). ^{19}F-{H} NMR (C_3D_6O, 223K): δ (ppm), **4A** -108.56 (m, F_{ortho}, 2), -27.25 (s+d, F_{SCF3}, $^3J_{Pt\text{-}F}$ = 96.63 Hz, 3) **4B** -108.64 (m, F_{ortho}, 2), -27.64 (s+d, F_{SCF3}, $^3J_{Pt\text{-}F}$ = 93.01 Hz, 3). Anal. Calcd. for $C_{16}H_{12}F_8PtS_4$: C 28.28; H 1.78; S 18.87. Found: C 28.1; H 1.5; S 18.7.

$[Pt(SCF_3)_2(4\text{-}C_6H_4FSCH_2CH_2SC_6H_4F\text{-}4)]$ 5. Yellow solid, Yield: 179 mg (88%). ^{19}F-{H} NMR (C_3D_6O, 296K): δ (ppm) -108.5 (m, F_{para}, 2), -26.98 (s+d, F_{SCF3}, $^3J_{Pt\text{-}F}$ = 89.11 Hz, 3). ^{19}F-{H} NMR (C_3D_6O, 223 K): δ (ppm), **5A** -108.78(m, F_{ortho}, 2), -27.28 (s+d, F_{SCF3}, $^3J_{Pt\text{-}F}$ = 96.90 Hz, 3) **5B** -108.38(m, F_{ortho}, 2), -27.67 (s+d, F_{SCF3}, $^3J_{Pt\text{-}F}$ = 93.12 Hz, 3). Anal. Calcd. for $C_{16}H_{12}F_8PtS_4$: C 28.28; H 1.78; S 18.87. Found: C 28.3; H 1.4; S 18.6.

$[Pt(SCF_3)_2(3\text{-}C_6H_4(CF_3)SCH_2CH_2SC_6H_4(CF_3)\text{-}3)]$ 6. Yellow solid, Yield: 205 mg (88%). ^{19}F-{H} NMR (C_3D_6O, 296 K): δ (ppm) -62.43(m, F_{CF3}, 2), -27.06 (s+d, F_{SCF3}, $^3J_{Pt\text{-}F}$ = 94.83 Hz,

3). ^{19}F-{H} NMR (C_3D_6O, 223K): δ (ppm), **6A** -108.67(m, F_{ortho}, 2), -27.34 (s+d, F_{SCF3}, $^3J_{Pt\text{-}F}$ = 89.77 Hz, 3) **3B** -108.39(m, F_{ortho}, 2), -27.76 (s+d, F_{SCF3}, $^3J_{Pt\text{-}F}$ = 94.86 Hz, 3). Anal. Calcd. for $C_{18}H_{12}F_{12}PtS_4$: C 27.73; H 1.55; S 16.45. Found: C 27.5; H 1.3; S 16.6.

Crystallographic data. X-Ray diffraction data for compounds **3** and **4** were collected at room temperature with a Siemens P4 diffractometer and corrected for absorption effect on the basis of y-scans, using standard procedures [27]. The structures were solved by direct methods using SHELXS97 [28]. and least-squares refinements based on F^2 were carried out by full-matrix method of SHELXL97-2 [28]. All non-H atoms were refined with anisotropic displacement parameters, without geometric constraints or restraints. H atoms were placed in idealized positions [constrained distances: C-H = 0.93 Å for aromatic CH and 0.97 Å for methylene CH_2; Isotropic displacement parameters were fixed to U_{iso}(H)=1.2U_{eq}(carrier C atom)]. Complete structures have been deposited with the CCDC. Deposition number: 617514 for **3**, 617515 for **4**. Structure factors are available on request to authors. Artwork has been prepared using MERCURY (release 1.4.1) [19].

Acknowledgements

The financial support from DGAPA-UNAM-IN119305 and CONACYT-44494-Q are gratefully acknowledged.

References

1. Dance, I.G., *Polyhedron* **1986**, 5, 1037-1104.
2. Blower, J.P.; Dilworth, J.R. *Coord. Chem. Rev.* **1987**, 76, 121-185.
3. García, J.J.; Arévalo, A.; Montiel, V.; Del Río, F.; Quiroz, B.; Adams, H.; and Maitlis, P.M. *Organometallics* **1997**, *16*, 3216-3220.
4. Sellmann, D.; Hille, A.; Heinemam, F.W.; Moll, M.; Rösler, A.; Sutter, J.; Brehm, G.; Reiher, M.; Hess, B.A.; Schneider, S. *Inorganica Chimica Acta* **2003,** *348*, 194-198.
5. Krebs, B.; Henkel, G. *Angew. Chem. Int. Ed. Engl.* **1991**, *30*, 769-788.
6. (a) Imai, S.; Suzuki, S.K.; Fujisawa, K.; Moro-oka, Y. *J. Inorg. Biochem.* **1997,** *67*, 60. (b) Roach, M.P.; Franzen, S.; Dang, P.S.H.; Boxer, S.G.; Woodruff, W.H.; Dawson, J.H. *J. Inorg. Biochem.* **1997,** *67*, 134. (c) Ruppert, R.; Kreps, B.; Reedijk, J. *J. Inorg. Biochem.* **1995,** *59*, 336. (d) Tsagkalidis, W.; Rodewald, D.; Render, D. *J. Inorg. Biochem.* **1995,** *59*, 594.
7. (a) Clark, H.C.; Jain, V.K.; Rao, G.S. *J. Organomet. Chem.* **1985,** *279*, 181-191. (b) Jain, V.K.; Rao, G.S. *Inorg. Chim. Acta* **1987,** *127*, 161-167. (c) Clarke, M.L. *Polyhedron* **2001**, *20*, 151-164. (d) Karet, G.B.; Kostiæ, N.M. *Inorg. Chem.* **1998,** *37*, 1021-1027.
8. Torres-Nieto, J.; Arévalo, A.; García-Gutiérrez, P.; Acosta-Ramírez, A.; García, J.J. *Organometallics* **2004,** *23*, 4534-4536.
9. Torrens, H. *Coord. Chem. Rev.* **2000**, 196, 331-352.
10. a) Rivera, G.; Bernès, S.; Rodríguez de Barbarin, C.; Torrens, H. *Inorg. Chem.* **2001**, *40*, 5575-5580 b) Usón, R.; Forniés, J.; Usón, N.A.; Tomás, M.; Ibañez, M.A. *J. Chem. Soc. Dalton Trans.* **1994**, 401-405. c) Usón, R., Forniés, J.; Falvello, L.R.; Usón, M.A.; Usón, I., Herrero, S. *Inorg. Chem.* **1993**, *32*, 1066-1067.
11. Abel, E.W.; Bhargava, S.K.; Orrell, K.G. *Prog. Inorg. Chem.* **1984**, *32*, 1-118.
12. Cross, R.J.; Rycroft, D.S.; Sharp, D.W.A.; Torrens, H. *J. Chem. Soc., Dalton Trans.* **1980**, 2434-2441.
13. Shaver, A.; Morris, S.; Turrin, R.; Day, V.M. *Inorg. Chem.* **1990**, 29, 3622-3629.
14. Beck, W.; Tadros, S., *Z. Anorg Allg. Chem.* **1979**, 375, 231. Beck, W.; Stetter, K.H.; Tadros, S.; Schwarzhans, K.E. *Chem. Ber.* **1967**, 100, 3944-3949.
15. Cross, R.J.; Manojlovic-Muir, L.; Muir, K.W.; Rycroft, D.S.; Sharp, D.W.A.; Solomun, T.; Torrens, H. *J. Chem. Soc., Chem. Comm.* **1976**, 291-292.
16. Cross, R.J.; Dalgleish, I.G.; Smith, G.J.; Wardle, R. *J. Chem. Soc., Dalton Trans.* **1972**, 992-999.
17. Bautista, J.; Bertran, A.; Bernès, S.; Duran, U.; Torrens, H. *Rev. Soc. Quím. Méx.* **2003**, *47*, 44-52.
18. Dixon, K.R.; Moss, K.C.; Smith, M.A.R. *J. Chem. Soc., Dalton Trans.* **1973**, 1528-1532.
19. Bruno, I.J.; Cole, J. C.; Edgington, P. R.; Kessler, M.; Macrae, C. F.; McCabe, P.; Pearson, J.; Taylor, R. *Acta Cryst.* **2002**, *B58*, 389-397.
20. Vaska, L.; Peone, J. *Chem. Comm.* **1971**, 418-419.
21. Hunter, W.N.; Muir, K.W.; Sharp, D.W.A. *Acta Cryst.* **1984**, *C40*, 37-39.
22. Martin, E.; Toledo, B.; Torrens, H.; Lahoz, F.J.; Terreros, P. *Polyhedron* **1998**, 17, 4091-4099.
23. Cano, O.; Leal, J.; Quintana, P.; Torrens, H. *Inorg. Chim. Acta* **1984**, *89*, L9-L10.
24. a) Bertran, A.; del Rio, F.; Torrens, H. *Sulfur Lett.* **1992**, *15*, 11-17. b). Peach, M.E., *Can. J. Chem.* **1968**, *46*, 2699-2708. c) Bertran, A.; Garcia, J.; Martin, E.; Sosa, P.; Torrens, H. *Rev. Soc. Quím. Méx.* **1993**, *37*, 185-189.
25. Emeleus, H.J.; McDuffie, D.E., *J. Chem. Soc.* **1961**, 2597-2603
26. Riddick, J.A.; Bunger, W.B.; Sakaro, T.K., Organic Solvents: Physical Properties and Methods of Purification, 4ª Ed., Techniques of Chemistry, Vol II, Wiley-Interscience, N.Y. **1970**.
27. Sheldrick, G. M. SHELXS97 and SHELXL97. *Programs for Solution and Crystal Structure Refinement*, University of Göttingen, Göttingen, Germany, **1997**.
28. Siemens, XSCANS. Version 2.21. Siemens Analytical X-ray Instruments Inc., Madison, Wisconsin, USA, **1996**.